RESEARCH

Association of *PPARGC1A* gene polymorphism and mtDNA methylation with coal-burning fluorosis: a case–control study

Juhui Song[1†], Ansu Zhao[1†], Ruichao Li[1,2], Yunyan Luo[1], Yangting Dong[1], Chanjuan Wang[1], Ting Zhang[1], Jie Deng[1], Xiaolan Qi[1], Zhizhong Guan[1] and Yan He[1*]

Abstract

Background Coal-burning fluorosis is a chronic poisoning resulting from the prolonged use of locally available high-fluoride coal for heating and cooking. Prolonged fluoride exposure has been demonstrated to decrease PPARGC1A levels. Therefore, this case-control aims to evaluate the genetic association of PPARGC1A gene polymorphisms and methylation of the mitochondrial D-loop region with coal-burning fluorosis.

Result The results showed that the TT genotype at rs13131226 and the AA genotype at rs1873532 increased the risk of coal-burning fluorosis ($OR = 1.84$, $P = 0.004$; $OR = 1.97$, $P = 0.007$), the CT and CC genotypes at rs7665116 decreased the risk of coal-burning fluorosis ($OR = 0.54$, $P = 0.003$). The TT genotype at the rs2970847 site and the AA genotype at the rs2970870 site increase the risk of developing skeletal fluorosis ($OR = 4.12$, $P = 0.003$; $OR = 2.22$, $P = 0.011$). Haplotype AG constructed by rs3736265-rs1873532 increased the risk of the prevalence of coal-burning fluorosis ($OR = 1.465$, $P = 0.005$); CG decreased the risk of the prevalence of coal-burning fluorosis ($OR = 0.726$, $P = 0.020$). Haplotype CGGT constructed by rs6821591-rs768695-rs3736265-rs2970847 increased the risk of the prevalence of skeletal fluorosis ($OR = 1.558$, $P = 0.027$). A 1% increase in CpG_4 methylation levels in the mtDNA D-loop region is associated with a 2.3% increase in the risk of coal-burning fluorosis. Additionally. There was a significant interaction between rs13131226 and rs1873532; CpG_4 and CpG_8.9; rs13131224,rs6821591 and rs7665116 were observed in the occurrence of fluorosis in the Guizhou population ($\chi^2 = 16.917$, $P < 0.001$; $\chi^2 = 21.198$, $P < 0.001$; $\chi^2 = 36.078$, $P < 0.001$).

Conclusion PPARGC1A polymorphisms rs13131226 and rs1873532 and the mitochondrial DNA D-loop methylation site CpG_4 have been associated with an increased risk of fluorosis, conversely polymorphism rs7665116 was associated with a decreased risk of fluorosis. Polymorphisms rs2970870 were associated with increased risk of skeletal fluorosis, and polymorphism rs2970847 was associated with decreased risk of skeletal fluorosis. These SNPs and CpG can be used as potential targets to assess fluorosis risk.

Keywords Cola-burning fluorosis, PPARGC1A, Genepolymorphism, Mitochondrial DNA methylation

[†]Juhui Song and Ansu Zhao contributed equally to this work.

*Correspondence:
Yan He
annieheyan@gmc.edu.cn
[1]Key Laboratory of Endemic and Ethnic Diseases, Ministry of Education
& Key Laboratory of Medical Molecular Biology of Guizhou Province, &

Collaborative Innovation Center for Prevention and Control of Endemic and Ethnic Regional Diseases Co-constructed by the Province and Ministry, Guizhou Medical University, Guiyang, Guizhou, China
[2]Department of Laboratory Medicine, Guangzhou Panyu Central Hospital, Guangzhou, China

Background

The human body requires trace amounts of fluoride for normal growth and development [1]. However, excessive fluoride intake can lead to tissue, organ and systemic damage. Endemic fluorosis, abbreviated as fluorosis, is a chronic systemic condition resulting from elevated fluoride levels in the local environment of a specific region, which may, in turn, cause prolonged excessive fluoride consumption among the population residing in that area [2]. Fluorosis primarily manifests as dental fluorosis, characterized by mottled teeth, and skeletal fluorosis (SF), which presents with disabling deformities, osteoporosis and osteosclerosis [3, 4]. On the other hand, coal-burning fluorosis (fluorosis) is a chronic poisoning resulting from the prolonged use of locally available high-fluoride coal for heating and cooking. In China, approximately 16.5 million individuals suffer from coal-burning fluorosis due to the indoor combustion of fluoride-rich coal for heating and food preparation [5].

Mitochondrial biosynthesis is a vital life process responsible for the maintenance and repair of mitochondrial function within an organism [6]. This process, known as mitochondrial biogenesis, regulates mitochondrial mass in response to energy requirements [7]. Successful mitochondrial biogenesis requires close coordination between the nuclear and mitochondrial genomes, and any impairment in this process can result in mitochondrial dysfunction, contributing to the onset of various diseases [8]. There is compelling evidence linking the toxic effects of environmental pollutants to the mitochondrial biosynthetic pathway [9]. For instance, it has been found that the Peroxisome proliferator-activated receptor γ coactivator 1α (*PPARGC1A*) plays a pivotal role as a major regulator of genes involved in both energy metabolism and mitochondrial biosynthesis [10]. It serves as a co-transcriptional regulator that increases the expression level and activity of NRF1 and NRF2 by interacting with two key nuclear transcription factors, nuclear respiratory factors 1 and 2 (NRF1 and NRF2), and through protein-protein interactions. NRF1 and NRF2 play essential roles in activating mitochondrial transcription factor A (Tfam) and binding to the promoter region of nuclear genes responsible for encoding the five subunits of the mitochondrial electron transport chain (ETC) [11]. This activation enhances the assembly of the respiratory apparatus and regulates various processes, including heme biosynthesis, import of nuclear-encoded mitochondrial proteins, and mtDNA replication and transcription, leading to the induction of mitochondrial biogenesis [12]. Studies have demonstrated that prolonged exposure to fluoride results in reduced levels of *PPARGC1A* and an increase in acetylated *PPARGC1A* levels [13]. Accumulating data indicate that fluoride generally hampers mitochondrial biogenesis and decreases mitochondrial numbers in most tissues [12]. Single nucleotide polymorphism (SNP) refers to a DNA sequence polymorphism resulting from a variation in a single nucleotide at a specific genomic DNA site. In recent years, an increasing number of SNPs associated with fluorosis have been documented [14]. However, there is limited research on the connection between polymorphisms in the *PPARGC1A* gene and susceptibility to fluorosis within the population.

DNA methylation is one of the most common early epigenetic modifications, and it also affects mitochondrial DNA (mtDNA), suggesting that mtDNA methylation may impact mitochondrial function [15]. The mitochondrial D-loop region (D-loop), the only non-coding region in mtDNA, plays a crucial role as it contains the starting points for mtDNA replication and transcription and is an essential regulatory region for these processes [16]. Several studies have shown that the methylation of the D-loop region can be influenced by various environmental factors [17, 18]. For instance, individuals exposed to arsenic in their drinking water exhibit changes in D-loop region methylation, which can subsequently affect the number of mtDNA copies [19]. Moreover, there is evidence indicating that epigenetic changes induced by fluoride exposure can contribute to the development of fluorosis [20].

Until now, there has been limited research on the association between *PPARGC1A* gene polymorphisms and methylation of the mitochondrial D-loop region in relation to fluorosis. Therefore, we designed this present study using a case-control study approach to examine 16 SNPs within the *PPARGC1A* gene genotyping and mitochondrial D-ring methylation levels, utilizing MassARRAY SNP and MassARRAY EpiTYPER (Agena Bioscience, Inc.). These analyses were performed to assess both mitochondrial D-loop region methylation levels and the genetic relationship between *PPARGC1A* gene polymorphisms and Guizhou fluorosis, with the aim to provide valuable insights into the genetic pathogenesis of fluorosis, as well as prevention and control strategies.

Results

Analysis of basic information in the population

In both the fluorosis group and the control group, there were no statistically significant differences in age between the two groups ($P>0.05$). However, statistically significant differences were observed in gender, BMI and literacy levels between the two groups ($P<0.05$). Specifically, the BMI of individuals in the fluorosis group was higher than that in the control group. Additionally, in the subgroups of non-SF and SF, statistically significant differences in BMI were observed ($P<0.05$), with the Weight of individuals in the non-SF group being higher than that in the SF group. The age difference of methylation subjects was

Song *et al. BMC Genomics*   (2024) 25:908

Page 3 of 10

not statistically significant (*P*>0.05). Given the substantial correlation between the extent of DNA methylation and advancing age, the absence of a significant age disparity within the two cohorts suggests the viability of the research protocol.(Table 1 and additional file 1: Table S1).

Allele and genotype distribution

In both the control and fluorosis groups, the distribution of all SNPs in the control group adhered to the Hardy-Weinberg equilibrium (*P*<0.05). However, the distribution of the rs1873532 site in both the non- SF and SF groups deviated from the Hardy-Weinberg equilibrium (*P*>0.05) and was consequently excluded from subsequent analyses. Comparison of the differences in allele and genotype frequencies of various SNPs in different populations revealed statistically significant differences in the distribution of alleles and genotypes of the *PPARGC1A* gene at SNPs rs13131226, rs1873532 and rs7665116 between the fluorosis and control groups (*P*<0.05). Similarly, differences in the distribution of alleles and genotypes of the *PPARGC1A* gene at SNPs rs13131226, rs2970847 and rs2970870 were also statistically significant between the non-SF and SF groups (*P*<0.05) (Additional file 2: Table S2).

Genetic pattern analysis

Genetic pattern analysis of the rs13131226, rs1873532 and rs7665116 SNPs associated with fluorosis was conducted using binary logistic regression analysis, with adjustments for confounding factors, including sex, BMI and culture. In both the control and fluorosis populations, the results indicated that the rs13131226 site's CT and CC genotypes were associated with an increased risk of fluorosis compared to the TT genotype (OR=1.84, 95% CI: 1.21–2.80, *P*=0.004), while the rs1873532 site's AA genotype was more likely to be associated with an increased risk of fluorosis compared to the CC or CA genotypes (OR=1.97, 95% CI: 1.18–3.29, *P*=0.007). Conversely, for the rs7665116 site, the CT and CC genotypes were associated with a decreased risk of fluorosis

compared to the TT genotype (OR=0.54, 95% CI: 0.35–0.81, *P*=0.003). In the non-SF and SF groups, the TT genotype of the rs2970847 site increased the risk of developing fluorosis compared to the CC and CT genotypes (OR=4.12, 95% CI: 1.60-10.57, *P*=0.003), and the AA genotype of the rs2970870 site was associated with an increased risk of fluorosis compared to the GG and AG genotypes (OR=2.22, 95% CI: 1.21–4.08, *P*=0.011). Further details are shown in Additional file 3: Table S3.

Linkage disequilibrium and haplotype analysis

Linkage disequilibrium analysis for all SNPs was conducted using Haploview 4.2, and the results are presented in Fig. 1, which show the D' values used to indicate the degree of linkage disequilibrium, with D' = 0 indicating complete linkage equilibrium, D' = 1 indicating complete linkage disequilibrium, and D' > 0.8 indicating strong linkage disequilibrium, represented by red squares. The analysis revealed strong linkage disequilibrium in several SNP pairs in both the control and fluorosis groups, including rs6821591-rs768695, rs3736265-rs1873532, rs2305682-rs4469064-rs58990583 and rs2970870-rs3796407, as well as rs590183-rs614457(Figs. 1A). Similarly, strong linkage disequilibrium was observed in rs6821591-rs768695-rs3736265-rs2970847, rs58990583-rs2305682-rs4469064 and rs614457-rs590183 in the non-SF and SF groups (Fig. 1B). Haplotype analysis was conducted using SHEsis online software, and the results indicated that the haplotype AG, constructed from rs3736265-rs1873532, increased the risk of fluorosis prevalence (OR=1.465, 95% CI: 1.134–1.893, *P*=0.005) in both the control and fluorosis groups. Conversely, the haplotype CG decreased the risk of fluorosis prevalence (OR=0.726, 95% CI: 0.560–0.940, *P*=0.020). Additionally, the haplotype CGGT, constructed from rs6821591-rs768695-rs3736265-rs2970847, increased the risk of SF prevalence (OR=1.558, 95% CI: 1.051–2.311, *P*=0.027) in both the non- SF and SF groups (Table 2).

Methylation level of mtDNA D-loop region

As the methylation result data were skewed, the median (quartiles) was used to express the results, and the rank sum test was used for comparison between groups. The findings indicate a significant difference in the methylation levels of CpG_2, CpG_4, CpG_7 and overall methylation between the fluorosis group and the control group (z=-2.296, *P*=0.022; z=-2.354, *P*=0.019; z=-2.296, *P*=0.022, z=-2.518, *P*=0.012) (Table 3). CpG_2, CpG_4, CpG_7, and overall methylation levels were higher than those of the control group (Fig. 2).

Table 1 Basic characteristics of methylation research subjects

Variables		Control (*n* = 46)	Coal-burning fluorosis (*n* = 49)	χ²/t	*P*
Gender	Male	29(63.04)	19(38.78)	5.59	**0.018**
	Female	17(36.96)	30(61.22)		
Age		47.80 ± 14.80	49.18 ± 15.10	-0.449	0.654
Weight (kg)		56.48 ± 8.67	58.73 ± 12.91	1.936	0.168
Height (cm)		155.95 ± 8.05	155.81 ± 9.81	1.605	0.208
BMI (kg/m2)		23.22 ± 3.09	24.07 ± 4.28	87.135	0.272

Bold indicates *P*<0.05. Measurement data are expressed as mean±SD, and Student's t test is used for comparison between groups. Counting data are expressed as frequency (rate), and Chi-square test is used for comparison between groups
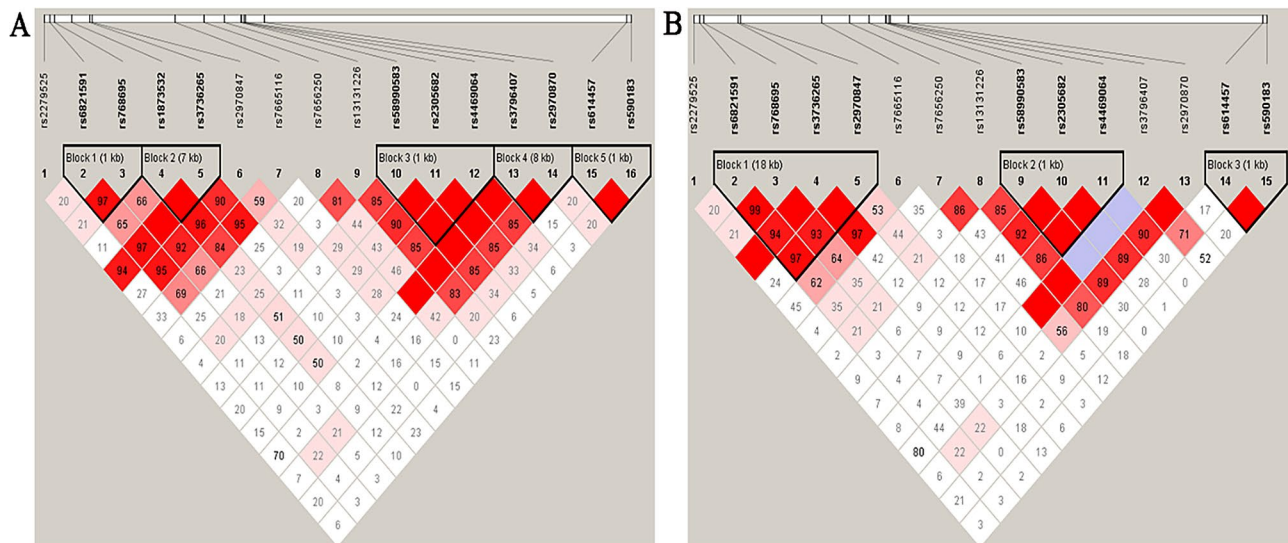
Fig. 1 *PPARGC1A* gene linkage disequilibrium analysis (*D*). **A** Linkage disequilibrium analysis of *PPARGC1A* gene in control and fluorosis groups. **B** Linkage disequilibrium analysis of *PPARGC1A* gene in non-SF and SF groups. D = 0 meant complete linkage equilibrium, D = 1 meant complete linkage disequilibrium, and > 0.8 meant strong linkage disequilibrium

Association between methylation of mitochondrial D-loop region and fluorosis

Binary logistic regression analysis of the methylation results, adjusted for gender, showed that for every 1% increase in the CpG_4 methylation level, there was a corresponding 2.3% increase in the likelihood of developing fluorosis (OR = 1.023, 95% CI: 1.001–1.045, *P* = 0.040) (Table 4).

Interaction analysis of *PPARGC1A* gene SNP with methylation in mitochondrial D-loop region

Analysis of the interaction effects involving SNP-SNP and CpG-CpG interactions was conducted using the MDR3.0.2 software to identify the best interaction models comprising 1–3 SNPs. The results found that the optimal combination of 2 SNP interactions between the fluorosis group and the control group was rs13131226-rs1873532, and the optimal combination of 3 SNP interactions was rs13131226-rs6821591-rs7665116. Cross-validation concordance was 8/10 in all cases, and both the training equilibrium accuracy and the test equilibrium accuracy were more than 50%, and the model was statistically significant ($\chi^2 = 9.444$, *P* = <0.001; $\chi^2 = 36.078$, *P* < 0.001), indicating that rs13131226 and rs1873532 influenced the occurrence of fluorosis in the Guizhou population. Likewise, an interaction between CpG_1 and CpG_8.9 was observed in relation to the occurrence of fluorosis in the population ($\chi^2 = 40.312$, *P* < 0.001). (Additional file 4: Table S4 and Fig. 3).

Discussion

Fluorosis caused by coal-fired activities in Guizhou Province results from the prolonged use of stoves lacking proper smoke exhaust systems by rural residents. The release of fluorine-containing soot during coal burning significantly contaminates indoor air and food, leading to the chronic accumulation of fluoride in the population residing in this environment, ultimately resulting in fluorosis [20]. While the etiology of fluorosis is well understood, its underlying pathogenesis remains elusive. Genetic polymorphisms have been documented to be associated with susceptibility to fluorosis. For instance, a cross-sectional study in Zhijin County (Guizhou Province, China) revealed an association between the PON1 rs662 polymorphism and fluorosis development [21]. Despite some progress in reducing the prevalence of fluorosis through improved stoves and health awareness, recent studies have shown that both indoor and outdoor air fluoride levels in endemic fluorosis wards in the Bijie County (Guizhou Province, China) area are significantly higher than in control areas [22]. This ongoing issue, with millions of confirmed cases of dental fluorosis [23], emphasizes the need for further research on genetic susceptibility genes for fluorosis.

Recent scientific investigations have confirmed the detrimental impact of fluoride exposure on mitochondrial function [24, 25]. The *PPARGC1A* gene is closely related to mitochondrial function and promotes the synthesis of mitochondrial proteins, mtDNA replication and transcription, and new mitochondrial biogenesis [26]. A study reported that *PPARGC1A* total mRNA and protein expression were reduced in NaF-treated SH-SY5Y cells, and animal experiments showed that the protein

Song *et al. BMC Genomics*   (2024) 25:908

Page 5 of 10

Table 2 Haplotype association analysis

Population	Haplotype	Group A [a] [n ()]	Group B [b] [n ()]	χ2	OR (95 CI)	P
Fluorosis group and Control group	TA[c]	256(65.3)	441(68.3)	1.156	1.122(0.857–1.470)	0.282
	CG[c]	129(32.9)	198(30.6)	0.717	0.891(0.680–1.167)	0.397
	AG[c]	149(38.2)	308(47.5)	8.041	1.465(1.134–1.893)	**0.005**
	CG[d]	163(41.8)	222(34.3)	5.438	0.726(0.560–0.940)	**0.020**
	CA[d]	78(20)	118(18.2)	0.509	0.891(0.648–1.224)	0.475
	TCA[e]	328(84.1)	557(86)	0.666	1.210(0.850–1.723)	0.414
	CTG[e]	62(15.9)	87(13.4)	1.21	0.826(0.580–1.176)	0.271
	GG[f]	195(50)	341(52.6)	0.671	1.111(0.864–1.429)	0.413
	GA[f]	35(9)	48(7.4)	0.113	0.811(0.514–1.278)	0.737
	AG[f]	160(41)	259(40)	0.813	0.957(0.741–1.236)	0.367
	TC[g]	190(48.7)	309(47.7)	0.104	0.959(0.746–1.234)	0.747
	GT[g]	158(40.5)	255(39.4)	0.137	0.953(0.787–1.231)	0.711
	GC[g]	42(10.8)	84(13)	1.099	1.234(0.832–1.829)	0.295
Non-SF group and SF group	CGGC[h]	12(6.6)	40(8.6)	0.724	0.749(0.384–1.460)	0.395
	CGGT[h]	52(28.2)	94(20.3)	4.910	1.558(1.051–2.311)	**0.027**
	TAAC[h]	30(16.3)	86(18.5)	0.413	0.861(0.545–1.359)	0.520
	TAGC[h]	87(47.2)	238(51.3)	0.819	0.854(0.605–1.205)	0.369
	TCA[i]	160(87)	397(85.6)	0.048	1.508(0.639–1.752)	0.827
	CTG[i]	24(13)	63(13.6)	0.048	0.945(0.571–1.566)	0.827
	TC[j]	95(51.6)	214(46.1)	1.603	1.247(0.886–1.755)	0.205
	GT[j]	64(34.8)	191(41.2)	2.248	0.762(0.534–1.087)	0.134
	GC[j]	25(13.6)	59(12.7)	0.089	1.079(0.653–1.784)	0.766

Bold indicates *P* < 0.05

[a]. Group A indicates control or non-SF group;

[b]. Group B indicates Fluorosis group or SF group;

[c]: Haplotype SNP combination rs6821591-rs768695 in control group and coal burning fluorosis group; [d]: Haplotype SNP combination rs11873532-rs3736265 in control group and coal burning fluorosis group; [e]: Haplotype SNP combination rs58990583-rs2305682-rs4469064 in control group and coal burning fluorosis group; [f]: Haplotype SNP combination rs3796407-rs2970870 in control group and coal burning fluorosis group; [g]: Haplotype SNP combination rs614457-rs590183 in control group and coal burning fluorosis group; [h]: Haplotype SNP combination rs6821591-rs768695-rs3736265-rs2970847 in non-SF group and SF group; [i]: Haplotype SNP combination rs58990583-rs2305682-rs4469064 in non-SF group and SF group; [j]: Haplotype SNP combination rs614457-rs590183 in non-SF group and SF group; All those frequency < 0.03 will be ignored in analysis

Table 3 Methylation levels of CpG sites in the D-loop region of mtDNA

CpG sites	Position	methylation level [Median, IQR (P25, P75)]		z	P
		Control (n = 46)	Fluorosis (n = 49)		
CpG_1	66 bp	0.41,0.59(0.44,0.85)	0.36, 0.65(0.51, 0.87)	-1.375	0.169
CpG_2	78 bp	0.13,0.17(0.08,0.25)	0.13, 0.20(0.13, 0.26)	-2.296	**0.022**
CpG_4	311 bp	0.20,0.36(0.05,0.41)	0.26, 0.34 (0.18,0.44)	-2.354	**0.019**
CpG_5	343 bp	0.03,0.06(0.05,0.08)	0.03, 0.07 (0.05,0.08)	-1.598	0.110
CpG_6	394 bp	0.02,0.02(0.02,0.04)	0.03,0.03(0.02,0.05)	-0.740	0.459
CpG_7	410 bp	0.13,0.17(0.08,0.25)	0.13, 0.20(0.13,0.26)	-2.296	**0.022**
CpG_8.9	432/437 bp	0.04,0.06(0.04,0.08)	0.03, 0.05 (0.04,0.07)	-0.477	0.634
Overall methylation levels		0.08,0.21(0.04,0.25)	0.12,0.25(0.06,0.31)	-2.518	**0.012**

Bold indicates $P<0.05$. Quantitative skewed data are represented by Median (IQR), and comparisons between groups are performed using the Mann–Whitney test
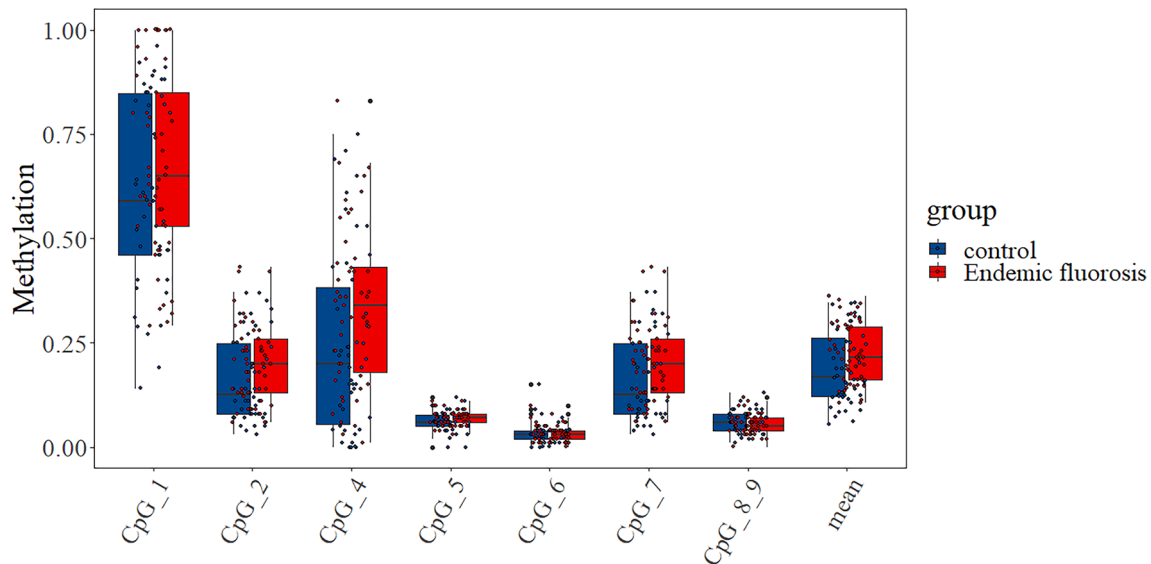

Fig. 2 Boxplot of methylation levels at CpG sites in the PPARGC1A gene (n = 95)

Table 4 Binary logistic regression analysis of the association between CpG and fluorosis

CpG	B	SD	WALD	OR	95CI[a]	P
CpG_1	0.010	0.009	1.197	1.010	0.992–1.029	0.274
CpG_2	0.038	0.023	4.116	1.039	0.994–1.086	0.092
CpG_4	0.022	0.011	4.217	1.023	1.001–1.045	**0.040**
CpG_5	0.136	0.104	1.711	1.145	0.935–1.403	0.191
CpG_6	0.020	0.090	0.049	1.020	0.855–1.218	0.824
CpG_7	0.038	0.023	2.839	1.039	0.994–1.086	0.092
CpG_8.9	-0.027	0.084	0.101	0.973	0.825–1.148	0.750

Bold indicates $P<0.05$

[a]: adjust sex

expression of *PPARGC1A* was reduced in NaF-exposed hippocampal neurons [27]. Learning memory capacity in rats with chronic fluorosis was negatively correlated with *PPARGC1A* water in serum, hippocampal and cortical brain tissues [28]. However, studies related to the association between *PPARGC1A* gene polymorphisms and susceptibility to coal-burning fluorosis in the population are rarely reported. Therefore, our case-control study explored the relationship between *PPARGC1A*

gene and susceptibility to fluorosis for the first time. We found that rs7665116 was associated with the occurrence of fluorosis in Guizhou population. The major T allele of rs7665116 was found to be associated with reduced iATP levels [29]. Reduced iATP levels are indicative for reduced cellular immunocompetence [30], which may lead to an increased risk of disease, confirming our findings. Regression analysis showed that carriers of the minor allele C had a reduced risk of fluorosis compared with
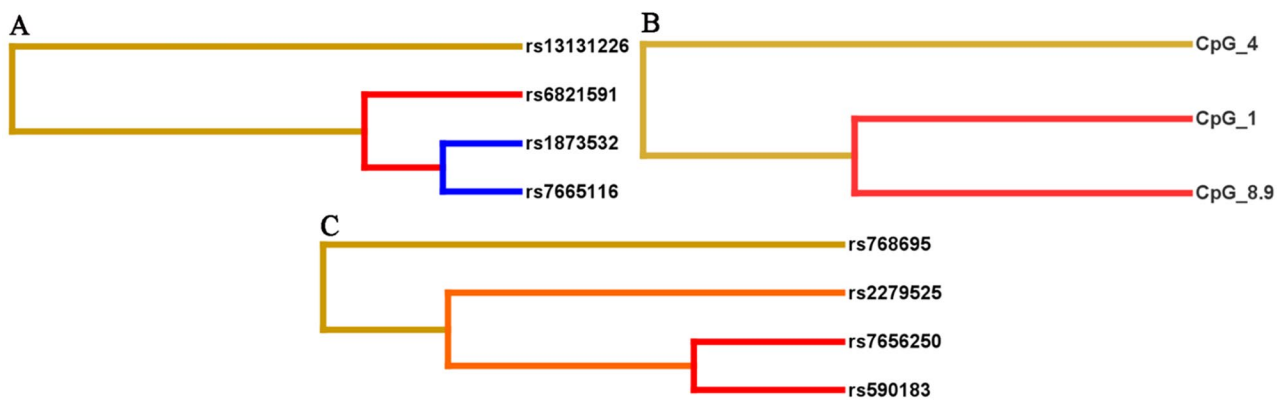
Fig. 3 Different types of interaction dendrogram for SNPs and CpG sites. **A** SNP-SNP interaction in control and fluorosis groups. **B** SNP-CpG interaction in control and fluorosis groups. **C** SNP-SNP interaction in Non-SF and SF groups. The dendrogram placed factors with strong interactions on the leaves. The color of the branches indicates the interaction from strong to weak (red, orange, green and blue). Red represents the highest degree of interaction or synergy, and blue represents low interaction or redundancy

carriers of the allele T. This change may lead to changes in iATP levels and thus influence the development of fluorosis. rs7665116 (chr4:23851388, T>C) is an intronic variant, and the intronic region affects gene function mainly by influencing splice site activity, which in turn affects gene translation and protein sequence. which in turn affects gene translation and protein sequence [31]. rs2970870 (chr4:23891394, A>G) is located in the promoter region of this gene, and we found that rs2970870 allele A is a protective factor for SF, and studies have shown that promoter SNP variants can alter gene function, affecting mRNA structure or stability and protein expression or function and other aspects [32]. Therefore, further comprehensive functional studies of rs7665116 and rs2970870 are needed. It has been reported that *PPARGC1A* plays a role in maintaining skeletal homeostasis, as evidenced by impaired skeletal structure in aged *PPARGC1A*-deficient mice [33]. Another study highlighted *PPARGC1A* as a potential therapeutic target for addressing osteoporosis and skeletal aging. It found that *PPARGC1A* deficiency in hematopoietic stem cells could be linked to osteoporosis and skeletal aging, with *PPARGC1A* deficiency promoting adipogenesis in hematopoietic stem cells at the expense of osteogenesis [34]. Specifically, rs2970870 were associated with increased risk of skeletal fluorosis, and polymorphism rs2970847 was associated with decreased risk of SF. Our study suggests that sequence variation in the *PPARGC1A* gene may play a role in the development of SF.

DNA methylation is a key epigenetic modification that can be influenced by various environmental factors, thereby affecting gene expression and potentially contributing to various phenotypic changes and diseases [35]. In particular, the D-loop region of the mitochondrial genome plays a crucial role in regulating mtDNA replication, transcription and organization, and it can

also be influenced by environmental factors, leading to changes in methylation levels [36]. Further studies found that CpG_4 of the target sequence was associated with fluorosis. Regression analysis after adjusting for confounders showed that every 1% increase in CpG_4 methylation level increased the risk of developing fluorosis by 2.3%, which could be attributed to methylation induced alterations in transcription factor binding sites, which ultimately affects mitochondrial biosynthesis and leads to fluorosis [37, 38].Disease onset and progression often result from the interplay of multiple SNPs or genes rather than a single genetic site [39]. Genetic susceptibility is typically inherited as a haplotype, and gene-gene interactions can have various effects on the phenotype [40]. Analyzing individual SNPs alone may capture only some significant SNPs and overlook their interactions. Therefore, SNP interaction analysis is a more effective approach to elucidate genetic mechanisms [41]. MDR interaction analysis revealed interactions between rs13131226 and rs1873532, as well as between rs13131226, rs6821591 and rs7665116 in the development of fluorosis. Although our study did not find a direct association between rs6821591 and fluorosis, it is possible that rs6821591 collaborated with other SNPs, collectively influencing the occurrence of fluorosis. Further investigation is warranted to better understand their interaction mechanisms.

In conclusion, this study represents the first attempt, to our knowledge, to explore the relationship between *PPARGC1A* SNP, mtDNA D-loop region methylation, and fluorosis using the MassArray technique. These findings provide valuable insights into the genetic underpinnings of fluorosis and may inform future prevention and control strategies. Moreover, the results of this study could be used as a theoretical basis for identifying individuals at higher risk for fluorosis.

This study has several limitations. First, most of the lifestyle-related information was obtained by questioning patients, and thus recall bias may be present. Second, these findings may only apply to people suffering from fluorosis in Guizhou. There is a need for more in-depth studies with more subjects from different regions and the whole PPARGC1A genotyping.

Objects and methods
Objects of the study
This study was conducted in adult populations from two regions in Guizhou Province: Bijie City, known for coal-fired pollution and fluorosis, and Changshun County, an area without such pollution. Their fluorosis status was determined based on the Diagnostic Criteria for Endemic Fluorosis (WS 192–2008) and the Diagnostic Criteria for Dental Fluorosis (WS/T 208–2011) issued by the National Health Commission of the People's Republic of China in 2008 and 2011, respectively. Participants were grouped according to their fluorosis status, based on which 324 individuals were identified for the fluorosis group and 195 for the control group. Within the fluorosis group, we further categorized individuals into those non-SF ($n=232$) and those with SF ($n=92$). Data were collected through questionnaires and on-site physical examinations to obtain information on gender, age, education, marital status, smoking, alcohol consumption, height, weight, and calculated body mass index (BMI; calculated using the formula: BMI=kg/m^2). All participants signed informed consent, and this study was reviewed and approved by the Human Trial Ethics Committee of Guizhou Medical University [Ethics 2019 No. (18)].

Screening criteria
The inclusion criteria for this study required that all participants were local residents born and raised in the study area. Exclusion criteria involved excluding individuals with major illnesses or incomplete survey data. Individuals who smoked more than one cigarette per day for at least one year were categorized as smokers, while those who consumed alcohol at least once per week for over one year were considered alcohol drinkers.

Biological sample collection
Approximately 5 ml of peripheral venous blood was obtained from study participants with their informed consent. The blood was collected in EDTA-Na2 anticoagulant tubes, transferred to cryopreservation tubes, and stored at -80 ℃ for further analysis.

Methods
DNA extraction, quantitative standardization and quality control
Genomic DNA was extracted from whole blood samples using a DNA extraction kit (Beijing Tiangen Biochemical Technology Co., Ltd.). The concentration and purity of the extracted DNA were assessed using a NanoDrop2000 Nucleic Acid Quantification Instrument (Thermo Fisher Scientific Inc.), ensuring an OD260/OD280 ratio between 1.8 and 2.0. The difference in concentration between duplicate wells was controlled to be within 5. The DNA was then labeled and organized in a 96-well plate, with each well theoretically containing 30 ng/μL of DNA in a 30 μL volume. These plates were sealed with sterile, enzyme-free film and stored in a medical cryopreservation box at -40 ℃ for subsequent analysis.

SNP selection and primer design and synthesis
We conducted a search on the NCBI database (https://www.ncbi.nlm.nih.gov/) and the Ensembl database (https://www.ensembl.org/index.html) to identify SNPs with a minimum allele frequency (MAF) greater than 5. Subsequently, we selected the SNPs that met this criterion. The design of primers for multiple SNP sites was evaluated using Assay Designer 4.0 software from Agena, with adjustment of design parameters based on different site information to ensure optimization. For each SNP site, three primers were synthesized using the PAGE primer purification method, consisting of two PCR primers and one single-base extension primer, as detailed in Table S5.

Methylation quantification of mtDNA D-loop region
To quantify the methylation of the mtDNA D-loop region, we used Massarray DNA methylation quantification technology. We obtained the complete sequence of the human mitochondrial genome (NC_012920.1) from the NCBI database and extracted the mitochondrial D-loop region sequence (16024.16569, 1.576). Primer design for this region was conducted using the EpiDesigner software. The appropriate primer scheme was selected in accordance with the software's recommendations (Table S5).

Genotyping and methylation detection
The MassARRAY detection platform was used to sequentially perform PCR amplification reaction, shrimp alkaline phosphatase reaction, single base extension reaction (for SNP detection) or transcriptase digestion reaction (for methylation detection), resin purification, microarray spotting and mass spectrometry analysis. Subsequently, the TYPER 4.0 software (Agena Bioscience, Inc.) was used to collect and compile the raw data, genotyping maps, and other detection results. Notably, CpG sites

Song *et al. BMC Genomics*   (2024) 25:908

Page 9 of 10

located between two adjacent base A or within small fragments generated by enzymatic cleavage share the same molecular weight. Therefore, these CpG sites were combined, resulting in the calculation of the average methylation level for this group of CpG sites. In this context, CpG_8 and CpG_9 were detected and treated as a single unit for analysis.

Statistical methods

Data analysis was conducted using SPSS version 26.0 (IBM Corp., Armonk, NY, USA). Normally distributed measurements are presented as mean±standard deviation (mean±sd) and compared using t-tests for intergroup comparisons. Skewed measurements are represented as [Median, IQR (P25, P75)] and analyzed for intergroup differences using Mann-Whitney tests. Count-based data are shown as frequency (constitutive ratio) and compared between groups using the chi-square test or Fisher's exact test. The association between SNPs and fluorosis was examined through binary logistic regression. Allele and genotype frequencies, as well as the Hardy-Weinberg equilibrium test, were computed using SNPStats online software (https://snpstats.net/start.htm). Linkage disequilibrium analysis was conducted using Haploview 4.2. Haplotype construction and the calculation of odds ratios (OR) and 95 confidence intervals (CI) were performed using the SHEsis online software (http://analysis.bio-x.cn/). Further analysis of SNPs was conducted using binary logistic regression. The MDR 3.0.2 software was used to explore SNP-SNP and CpG-CpG interactions. Methylation results were visualized using the R software (version 3.6.2, R Foundation for Statistical Computing, Vienna, Austria). Statistical significance was determined using a two-sided test, with $P<0.05$ indicating a significant difference.

Abbreviations

D-loop	D-loop region
ETC	Electron Transport Chain
Fluorosis	Coal-Burning Fluorosis
iATP	Intracellular Adenosine Triphosphate
mtDNA	Mitochondrial DNA
Non-SF	Non Skeletal Fluorosis
PPARGC1A	Peroxisome Proliferator-Activated Receptor γ Coactivator 1α
SF	Skeletal Fluorosis
SNP	Single Nucleotide Polymorphism

Supplementary Information

The online version contains supplementary material available at https://doi.org/10.1186/s12864-024-10819-9.

Supplementary Material 1

Supplementary Material 2

Supplementary Material 3

Supplementary Material 4

Supplementary Material 5

Data availability
Availability of data and materialsThe datasets used and/or analyzed during the current study are available from the corresponding author on reasonable request..

Declarations

Ethics approval and consent to participate
This study was reviewed and approved by the Human Trial Ethics Committee of Guizhou Medical University [Ethics 2019 No. (18)] and all participants provided written informed consent in accordance with the Declaration of Helsinki.

Consent for publication
Not applicable.

Competing interests
The authors declare no competing interests.

References

1. Srivastava S, Flora SJS. Fluoride in drinking water and skeletal fluorosis: a review of the global impact. Curr Environ Health Rep. 2020;7(2):140–6. https://doi.org/10.1007/s40572-020-00270-9.
2. Alhusaini AM, Faddah LM, El Orabi NF, Hasan IH. Role of some natural antioxidants in the modulation of some proteins expressions against Sodium Fluoride-Induced Renal Injury. Biomed Res Int. 2018;20185614803. https://doi.org/10.1155/2018/5614803.
3. Quadri JA, Sarwar S, Sinha A, Kalaivani M, Dinda AK, Bagga A, Roy TS, Das TK, Shariff A. Fluoride-associated ultrastructural changes and apoptosis in human renal tubule: a pilot study. Hum Exp Toxicol. 2018;37(11):1199–206. https://doi.org/10.1177/0960327118755257.
4. Meenakshi, Maheshwari RC. Fluoride in drinking water and its removal. J Hazard Mater. 2006;137(1):456–63.
5. de Oliveira MR, Nabavi SF, Manayi A, Daglia M, Hajheydari Z, Nabavi SM. Resveratrol and the mitochondria: from triggering the intrinsic apoptotic pathway to inducing mitochondrial biogenesis, a mechanistic view. Biochim Biophys Acta. 2016;1860(4):727–45. https://doi.org/10.1016/j.bbagen.2016.01.017.
6. Weinberg JM. Mitochondrial biogenesis in kidney disease. J Am Soc Nephrol. 2011;22(3):431–6. https://doi.org/10.1681/asn.2010060643.
7. Johnson J, Mercado-Ayon E, Mercado-Ayon Y, Dong YN, Halawani S, Ngaba L, Lynch DR. Mitochondrial dysfunction in the development and progression of neurodegenerative diseases. Arch Biochem Biophys. 2021;702:108698. https://doi.org/10.1016/j.abb.2020.108698.
8. Dabrowska A, Venero JL, Iwasawa R, Hankir MK, Rahman S, Boobis A, Hajji N. PGC-1α controls mitochondrial biogenesis and dynamics in lead-induced neurotoxicity. Aging. 2015;7(9):629–47. https://doi.org/10.18632/aging.100790.
9. Popov LD. Mitochondrial biogenesis: an update. J Cell Mol Med. 2020;24(9):4892–9. https://doi.org/10.1111/jcmm.15194.

10. Jornayvaz FR, Shulman GI. Regulation of mitochondrial biogenesis. Essays Biochem. 2010;47:69–84. https://doi.org/10.1042/bse0470069.

11. Li PA, Hou X, Hao S. Mitochondrial biogenesis in neurodegeneration. J Neurosci Res. 2017;95(10):2025–9. https://doi.org/10.1002/jnr.24042.

12. Avila-Rojas SH, Aparicio-Trejo OE, Sanchez-Guerra MA, Barbier OC. Effects of fluoride exposure on mitochondrial function: Energy metabolism, dynamics, biogenesis and mitophagy. Environ Toxicol Pharmacol. 2022;94:103916. https://doi.org/10.1016/j.etap.2022.103916.

13. Gao Y, Liu Y, Jiang Y, Qin M, Guan Z, Gao Y, Yang Y. Association between polymorphism and haplotype of ATP2B1 gene and skeletal fluorosis in Han population. Int J Environ Health Res 2023:1–11https://doi.org/10.1080/09603123.2023.2213159

14. Stoccoro A, Coppedè F. Mitochondrial DNA methylation and human diseases. Int J Mol Sci. 2021;22(9). https://doi.org/10.3390/ijms22094594.

15. Pastukh VM, Gorodnya OM, Gillespie MN, Ruchko MV. Regulation of mitochondrial genome replication by hypoxia: the role of DNA oxidation in D-loop region. Free Radic Biol Med. 2016;96:78–88. https://doi.org/10.1016/j.freeradbiomed.2016.04.011.

16. Janssen BG, Byun HM, Gyselaers W, Lefebvre W, Baccarelli AA, Nawrot TS. Placental mitochondrial methylation and exposure to airborne particulate matter in the early life environment: an ENVIRONAGE birth cohort study. Epigenetics. 2015;10(6):536–44. https://doi.org/10.1080/15592294.2015.1048412.

17. Xu Y, Li H, Hedmer M, Hossain MB, Tinnerberg H, Broberg K, Albin M. Occupational exposure to particles and mitochondrial DNA - relevance for blood pressure. Environ Health. 2017;16(1):22. https://doi.org/10.1186/s12940-017-0234-4.

18. Sanyal T, Bhattacharjee P, Bhattacharjee S, Bhattacharjee P. Hypomethylation of mitochondrial D-loop and ND6 with increased mitochondrial DNA copy number in the arsenic-exposed population. Toxicology. 2018;408:54–61. https://doi.org/10.1016/j.tox.2018.06.012.

19. Daiwile AP, Tarale P, Sivanesan S, Naoghare PK, Bafana A, Parmar D, Kannan K. Role of fluoride induced epigenetic alterations in the development of skeletal fluorosis. Ecotoxicol Environ Saf. 2019;169:410–7. https://doi.org/10.1016/j.ecoenv.2018.11.035.

20. Qin X, Wang S, Yu M, Zhang L, Li X, Zuo Z, Zhang X, Wang L. Child skeletal fluorosis from indoor burning of coal in southwestern China. J Environ Public Health. 2009;2009(969764). https://doi.org/10.1155/2009/969764.

21. Tao N, Li L, Chen Q, Sun Z, Yang Q, Cao D, Zhao X, Zeng F, Liu J. Association between antioxidant nutrients, oxidative stress-related gene polymorphism and skeletal fluorosis in Guizhou, China. Front Public Health. 2022;10849173. https://doi.org/10.3389/fpubh.2022.849173.

22. Wang X, Ming J, Qiu B, Liao Y, Liao Y, Wei S, Tu C, Pan X. Relationships between fluoride exposure, degree of bone phase damage, and bone formation markers in patients with coal combustion-contaminated fluorosis(in Chinese). J Appl Ecol. 2019;30(01):43–8. https://doi.org/10.13287/j.1001-9332.201901.026.

23. Guo J, Wu H, Zhao Z, Wang J, Liao H. Review on Health impacts from domestic coal burning: emphasis on endemic fluorosis in Guizhou Province, Southwest China. Rev Environ Contam Toxicol. 2021;258:1–25. https://doi.org/10.1007/398_2021_71.

24. Zhao Q, Niu Q, Chen J, Xia T, Zhou G, Li P, Dong L, Xu C, Tian Z, Luo C, et al. Roles of mitochondrial fission inhibition in developmental fluoride neurotoxicity: mechanisms of action in vitro and associations with cognition in rats and children. Arch Toxicol. 2019;93(3):709–26. https://doi.org/10.1007/s00204-019-02390-0.

25. Suzuki M, Everett ET, Whitford GM, Bartlett JD. 4-phenylbutyrate mitigates Fluoride-Induced cytotoxicity in ALC cells. Front Physiol. 2017;8302. https://doi.org/10.3389/fphys.2017.00302.

26. Fontecha-Barriuso M, Martin-Sanchez D, Martinez-Moreno JM, Monsalve M, Ramos AM, Sanchez-Niño MD, Ruiz-Ortega M, Ortiz A, Sanz AB. The role of PGC-1α and mitochondrial Biogenesis in kidney diseases. Biomolecules. 2020;10(2).

27. Zhao Q, Tian Z, Zhou G, Niu Q, Chen J, Li P, Dong L, Xia T, Zhang S, Wang A. SIRT1-dependent mitochondrial biogenesis supports therapeutic effects of resveratrol against neurodevelopment damage by fluoride. Theranostics. 2020;10(11):4822–38. https://doi.org/10.7150/thno.42387.

28. Liu X, Chen D, Qi X,Wu C,Li Y, Song H. Correlation between learning memory ability and PGC-1α levels in serum, hippocampus and cortical brain tissue in rats with chronic fluorosis(in Chinese). J GMU. 2018;43(10):1154–8. https://doi.org/10.19367/j.cnki.1000-2707.2018.10.007.

29. Haghikia A, Faissner S, Pappas D, Pula B, Akkad DA, Arning L, Ruhrmann S, Duscha A, Gold R, Baranzini SE, Malhotra S, Montalban X, Comabella M, Chan A. Interferon-beta affects mitochondrial activity in CD4 + lymphocytes: implications for mechanism of action in multiple sclerosis. Mult Scler. 2015;21(10):1262–70. https://doi.org/10.1177/1352458514561909.

30. Haghikia A, Perrech M, Pula B, Ruhrmann S, Potthoff A, Brockmeyer NH, Goelz S, Wiendl H, Lindå H, Ziemssen T, Baranzini SE, Käll TB, Bengel D, Olsson T, Gold R, Chan A. Functional energetics of CD4+-cellular immunity in monoclonal antibody-associated progressive multifocal leukoencephalopathy in autoimmune disorders. PLoS ONE. 2011;6(4):e18506. https://doi.org/10.1371/journal.pone.0018506.

31. Pagani F, Baralle FE. Genomic variants in exons and introns: identifying the splicing spoilers. Nat Rev Genet. 2004;5(5):389–96. https://doi.org/10.1038/nrg1327.

32. Wang B, Xu Q, Yang HW, Sun LP, Yuan Y. The association of six polymorphisms of five genes involved in three steps of nucleotide excision repair pathways with hepatocellular cancer risk. Oncotarget. 2016;7(15):20357–67. https://doi.org/10.18632/oncotarget.7952.

33. Colaianni G, Lippo L, Sanesi L, Brunetti G, Celi M, Cirulli N, Passeri G, Reseland J, Schipani E, Faienza MF, et al. Deletion of the transcription factor PGC-1α in mice negatively regulates bone Mass. Calcif Tissue Int. 2018;103(6):638–52. https://doi.org/10.1007/s00223-018-0459-4.

34. Yu B, Huo L, Liu Y, Deng P, Szymanski J, Li J, Luo X, Hong C, Lin J, Wang CY. PGC-1α controls skeletal stem cell fate and bone-fat balance in osteoporosis and skeletal aging by inducing TAZ. Cell Stem Cell. 2018;23(2):193–209. https://doi.org/10.1016/j.stem.2018.06.009.

35. Lim E, Xu H, Wu P, Posner D, Wu J, Peloso GM, Pitsillides AN, DeStefano AL, Adrienne Cupples L, Liu CT. Network analysis of drug effect on triglyceride-associated DNA methylation. BMC Proc. 2018;12(Suppl 9):27. https://doi.org/10.1186/s12919-018-0130-0.

36. Kim JI, Lee SY, Park M, Kim SY, Kim JW, Kim SA, Kim BN. Peripheral mitochondrial DNA Copy Number is increased in Korean attention-deficit hyperactivity disorder patients. Front Psychiatry. 2019;10:506. https://doi.org/10.3389/fpsyt.2019.00506.

37. Medvedeva YA, Khamis AM, Kulakovskiy IV, Ba-Alawi W, Bhuyan MS, Kawaji H, Lassmann T, Harbers M, Forrest AR, Bajic VB. Effects of cytosine methylation on transcription factor binding sites. BMC Genomics. 2014;15:119. https://doi.org/10.1186/1471-2164-15-119.

38. Cox LA, Nathanielsz PW. The importance of altered gene promoter methylation and transcription factor binding in developmental programming of central appetitive drive. J Physiol. 2009;587(Pt 20):4763–4. https://doi.org/10.1113/jphysiol.2009.181149.

39. Pei X, Liu L, Cai J, Wei W, Shen Y, Wang Y, Chen Y, Sun P, Imam MU, Ping Z, et al. Haplotype-based interaction of the PPARGC1A and UCP1 genes is associated with impaired fasting glucose or type 2 diabetes mellitus. Med (Baltim). 2017;96(23):e6941. https://doi.org/10.1097/md.0000000000006941.

40. Romao I, Roth J. Genetic and environmental interactions in obesity and type 2 diabetes. J Am Diet Assoc. 2008;108(4 Suppl 1):S24–28. https://doi.org/10.1016/j.jada.2008.01.022.

41. Chen Q, Mao X, Zhang Z, Zhu R, Yin Z, Leng Y, Yu H, Jia H, Jiang S, Ni Z, et al. SNP-SNP Interaction Analysis on Soybean Oil Content under multi-environments. PLoS ONE. 2016;11(9):e0163692. https://doi.org/10.1371/journal.pone.0163692.

Publisher's note